JOC The Journal of Organic Chemistry

ARTICLE

pubs.acs.org/joc

Time-Resolved Kinetic Study of the Electron-Transfer Reactions between Ring-Substituted Cumyloxyl Radicals and Alkylferrocenes. Evidence for an Inner-Sphere Mechanism

Massimo Bietti,*[,†] Gino A. DiLabio,*[,‡] Osvaldo Lanzalunga,*[,§] and Michela Salamone[†]

[†]Dipartimento di Scienze e Tecnologie Chimiche, Università "Tor Vergata", Via della Ricerca Scientifica, 1 I-00133 Rome, Italy

[‡]National Institute for Nanotechnology, National Research Council of Canada, 11421 Saskatchewan Drive, Edmonton, AB, Canada T6G 2M9

[§]Dipartimento di Chimica, Sapienza Università di Roma and Istituto CNR di Metodologie Chimiche (IMC−CNR), Sezione Meccanismi di Reazione, c/o Dipartimento di Chimica, Sapienza Università di Roma, P.le A. Moro, 5 I-00185 Rome, Italy

Supporting Information

ABSTRACT: A time-resolved kinetic study of the reactions of ring-substituted cumyloxyl radicals (4-X-CumO•: X = OMe, *t*-Bu, Me, Cl, CF_3) with methylferrocenes (Me_nFc: n = 2, 8, 10) has been carried out in acetonitrile solution. Evidence for an electron transfer (ET) process has been obtained for all radicals and an increase in reactivity has been observed on decreasing the oxidation potential of the ferrocene donor and on going from electron-releasing to electron-withdrawing ring substituents. Computations predict the formation of strongly bound π-stacked 4-X-CumO•/DcMFc complexes, characterized by intracomplex $\pi-\pi$ distances around 4 Å. These findings point toward a (nonbonded) inner-sphere ET mechanism for the reactions of the 4-X-CumO•/Me_nFc couples.

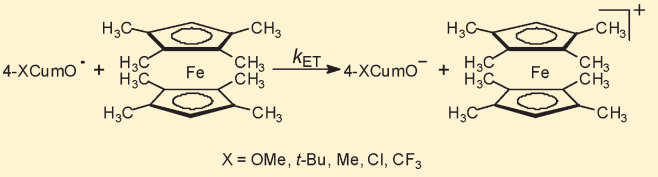

INTRODUCTION

The electron-transfer (ET) reactivity of organic free radicals has attracted considerable interest in recent years, with notable examples that include the study of the ET properties of peroxyl,[1−6] phenoxyl,[7−10] and *N*-oxyl radicals.[11−13] However, limited information is available on alkoxyl radicals,[14−16] one of the main classes of oxygen centered radicals. In this context, we have recently shown that the *tert*-butoxyl (*t*-BuO•), cumyloxyl (CumO•) and benzyloxyl (BnO•) radicals react with alkyl ferrocenes via an ET mechanism.[17] The results of our study led us to suggest that the ET reactions of BnO• and CumO• with ferrocene donors may not be described in terms of a straightforward outer-sphere ET mechanism. Computational modeling predicted the formation of π-stacked encounter complexes between the radicals and ferrocene donors. In these complexes, the alkoxyl radical aromatic ring can act as an electron relay shuttling the electron from the ferrocene to the formal oxygen atom radical center. This hypothesis was supported by the observation that, with *t*-BuO•, where this interaction is not possible, the ET rate constants for reaction with the ferrocene donors are at least 2 orders of magnitude lower than those measured for the corresponding reactions of BnO• and CumO•. This large difference in reactivity is present despite the relatively small differences in reduction potential between these three radicals, viz., $E^{\circ}_{RO\bullet/RO-}$ = −0.30, − 0.19, and − 0.10 V/SCE in acetonitrile for *t*-BuO•,[16c] BnO•,[17] and CumO•,[16a] respectively.

In order to probe the role of electronic effects on these ET processes and to obtain additional mechanistic information, we carried out a time-resolved kinetic study on the reactions of ring-substituted cumyloxyl radicals (4-X-CumO•: X = OMe, *t*-Bu, Me, Cl, CF_3) with a series of electron-rich methyl ferrocenes (Me_nFc), namely: 1,1′-dimethylferrocene (DMFc), 1,1′,2,2′,3,3′,4,4′-octamethylferrocene (OMFc), and decamethylferrocene (DcMFc), the structures for which are displayed in Chart 1. Computational modeling provides additional insights into the nature of the encounter complexes formed during the ET reactions.

RESULTS AND DISCUSSION

Ring-substituted cumyloxyl radicals (4-X-CumO•) were generated by 266 nm laser flash photolysis (LFP) of nitrogen saturated MeCN solutions (T = 25 °C) containing the parent *tert*-butyl 4-X-cumyl peroxides (eq 1).[18]

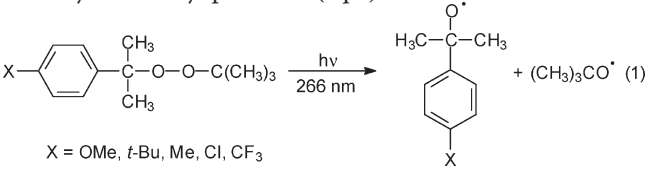

As described previously, in MeCN solution ring-substituted cumyloxyl radicals are characterized by a broad absorption band

Received: December 7, 2010
Published: February 24, 2011

   dx.doi.org/10.1021/jo102420p | *J. Org. Chem.* 2011, 76, 1789–1794

Chart 1

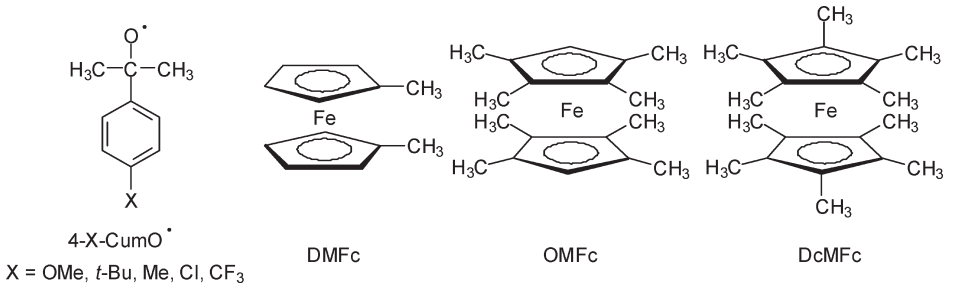

in the visible region of the spectrum whose position, as compared to the unsubstituted cumyloxyl radical for which λ_{max} (vis) = 485 nm,[19] is red-shifted by electron-donating (ED) ring substituents (X = OMe, Me) and blue-shifted by electron-withdrawing (EW) ones (X = Cl, CF_3).[19−21] Along this line, the time-resolved absorption spectrum observed after 266 nm LFP of *tert*-butyl 4-*tert*-butyl-cumyl peroxide, and displayed in the Supporting Information as Figure S1, is characterized by a visible absorption band with λ_{max} = 510 nm that is assigned to 4-*t*-Bu-CumO•. Under these conditions, the 4-X-CumO• radicals decay mainly by C−CH_3 β-scission, with rate constants that are not influenced to a significant extent by the nature of the ring substituent (k_β between 0.7 and 1.1 × 10^6 s^{-1}).[20] With 4-*t*-Bu-CumO•, the rate constant for C−CH_3 β-scission was measured following the decay of the visible absorption band at 510 nm as k_β = 7.7 × 10^5 s^{-1}.

The reactions of the 4-X-CumO• radicals with the ferrocene donors were studied in MeCN solution by LFP. Figure 1 shows the time-resolved absorption spectra observed after 266 nm LFP of a nitrogen-saturated MeCN solution (T = 25 °C) containing *tert*-butyl 4-chlorocumyl peroxide and DcMFc. The spectrum recorded 63 ns after the laser pulse (black circles) shows the characteristic 4-Cl-CumO• band centered at 500 nm.[20] The decay of this band (inset **b**), which is accelerated by the presence of DcMFc, is accompanied by a corresponding buildup of absorption at 270, 320, and 700 nm (insets **a** and **c**). Two isosbestic points can be identified at 410 and 580 nm. These absorption bands are assigned to the decamethylferrocenium ion ($DcMFc^+$) by comparison to literature data,[22] and to the spectrum observed previously after reaction between CumO• and DcMFc.[17]

The formation of $DcMFc^+$ clearly indicates the occurrence of an ET reaction from DcMFc to 4-Cl-CumO• (eq 2), in accordance with our previous observations of the analogous reaction involving the unsubstituted cumyloxyl radical.[17]

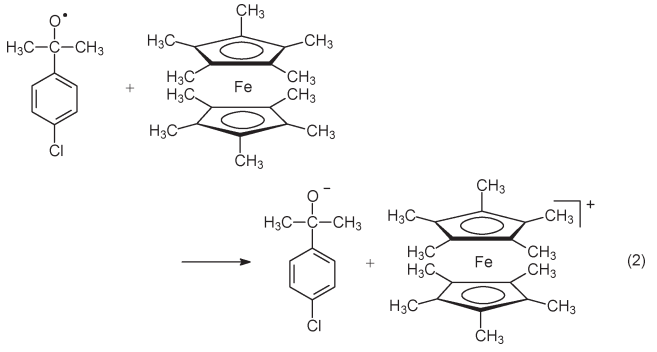

Analogous behavior was observed in the reactions of the 4-X-CumO• radicals with the ferrocene donors. In all cases the buildup of the pertinent ferrocenium ion bands was observed, indicating that ET reactions occurred. The time-resolved spectra observed after reaction of 4-Me-CumO• with OMFc are displayed in the Supporting Information (Figure S2).

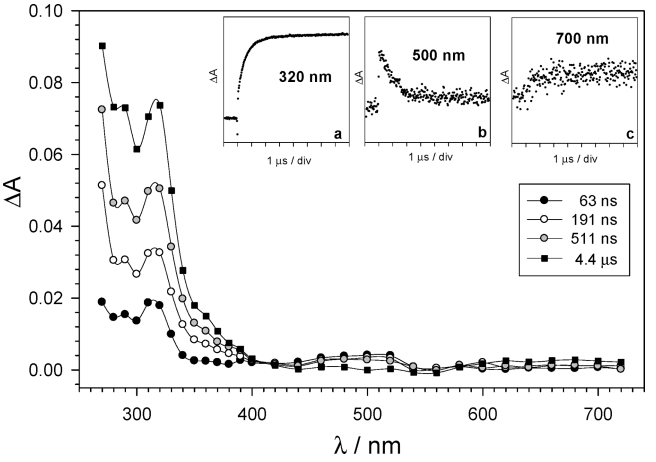

Figure 1. Time-resolved absorption spectra observed after 266 nm LFP of a nitrogen-saturated MeCN solution (T = 25 °C) containing *tert*-butyl 4-chlorocumyl peroxide (5.0 mM) and decamethylferrocene (0.19 mM) at 63 ns (black circles), 191 ns (white circles), 511 ns (gray circles), and 4.4 μs (black squares) after the 8 ns, 10 mJ laser pulse. Insets: (b) Decay of the 4-chlorocumyloxyl radical monitored at 500 nm. (a and c) Corresponding buildup of absorption at 320 (a) and 700 nm (c) assigned to the formation of the decamethylferrocenium ion.

Kinetic studies were carried out by LFP following the buildup of the ferrocenium ions between 300 and 330 nm and with 4-MeO-CumO•, characterized by the most intense visible absorption band among the series of cumyloxyl radicals investigated[19a,20,21] also by following the decay of this band at 580 nm.

Plots of the observed rate constants (k_{obs}) against [Me_nFc] produced excellent linear fits. The second-order rate constants for the one-electron oxidation of the ferrocene donors by 4-X-CumO• (k_2) were obtained from the slopes of these plots. All the kinetic data are collected in Table 1. For comparison, also included are the kinetic data obtained previously for CumO• and BnO•,[17] and the calculated solvent-phase (MeCN) electron affinities (EA) of the radicals. The plots of k_{obs} vs [Me_nFc] for the reactions of the 4-X-CumO• radicals are displayed in the Supporting Information (Figures S3−S15).

The data displayed in Table 1 show that k_2 increases with decreasing the oxidation potential of the ferrocene donor (0.29, − 0.02, and −0.10 V/SCE in MeCN for DMFc, OMFc, and DcMFc, respectively),[11c] as expected for an ET process. For

dx.doi.org/10.1021/jo102420p |*J. Org. Chem.* 2011, 76, 1789–1794

Table 1. Second-Order Rate Constants (k_2) for the Reactions of 4-X-CumO$^\bullet$ with Methylferrocenes (Me_nFc) Measured in MeCN at T = 25 °C[a] and Calculated Electron Affinities (EA) of the Radicals (kcal/mol)

	k_2/M^{-1} s^{-1}			
radical[b]	DMFc	OMFc	DcMFc	EA [c]
4-MeO-CumO$^\bullet$	*d*	1.3×10^9	2.4×10^9	104.6
	d	1.0×10^9 [e]	2.4×10^9[e]	
4-*t*-Bu-CumO$^\bullet$	*d*	1.6×10^9	*f*	103.3
4-Me-CumO$^\bullet$	*d*	1.6×10^9	3.2×10^9	104.8
CumO$^\bullet$ [g]	1.0×10^8	2.0×10^9	4.0×10^9	105.8
4-Cl-CumO$^\bullet$	1.3×10^8	3.3×10^9	5.4×10^9	106.6
4-CF_3−CumO$^\bullet$	1.9×10^8	4.2×10^9	7.4×10^9	107.4
BnO$^\bullet$ [g]	5.2×10^8	7.5×10^9	1.1×10^{10}	107.8

[a] Determined from the slope of the k_{obs} vs [Me_nFc] plots. Average of at least two values. Error <10%. k_{obs} was measured following the buildup of the pertinent ferrocenium ion (at 300 nm for $DMFc^+$, 330 nm for $OMFc^+$, and 320 nm for $DcMFc^+$). [b] Generated by 266 nm LFP of the parent *tert*-butyl 4-X-cumyl peroxides as described in eq 1. [c] Calculated using (RO)B3[23]LYP[24]/6-311+G(2d,2p)//B3LYP/6-31+G(d,p),[25] with the PCM[26] solvent model (MeCN), as implemented in Gaussian-03.[27] Zero-point energies (frequency scale factor = 0.9806) were used in the calculation of EAs. [d] The high concentrations of DMFc required for the kinetic study of the ET reactions prevented the determination of the corresponding second-order rate constants. [e] k_{obs} was measured following the decay of 4-MeO-CumO$^\bullet$ at 580 nm. [f] With 4-*t*-Bu-CumO$^\bullet$ the kinetic study was limited to the reaction with OMFc. [g] From ref 17.

CumO$^\bullet$, 4-Cl-CumO$^\bullet$, and 4-CF_3−CumO$^\bullet$, k_2 increases by a factor of ca. 40 on going from DMFc to DcMFc. Relative to the unsubstituted cumyloxyl radical CumO$^\bullet$, k_2 values increase for alkoxyl radicals with EW substituents (4-Cl and 4-CF_3) and decrease for those bearing ED substituents (4-Me, 4-*t*-Bu, and 4-MeO). Although the substituent effect is not very pronounced (k_2 values for OMFc and DcMFc are within a factor of 3 over the range of substituents), this behavior is in line with the oxidizing power of the ring-substituted cumyloxyl radicals that can be derived from the calculated solvent-phase (MeCN) electron affinity (EA) values displayed in Table 1.[28] This trend in k_2 is well matched by the EA values, as evidenced by the reasonably good correlations ($r^2 \geq 0.969$) obtained between log k_2 for the reactions of 4-X-CumO$^\bullet$ with OMFc and DcMFc and the EAs (see the Supporting Information, Figure S16). The slightly lower EA value obtained for 4-*t*-Bu-CumO$^\bullet$ may reflect poor differential treatment of the bulky substituent group by the implicit solvent model.

Figure 2 shows the plots of log k_2 against the Hammett σ substituent constant[29] for the reactions of 4-X-CumO$^\bullet$ with the three ferrocene donors. Good correlations ($r^2 \geq 0.973$) are observed in all cases, indicating that variations in rate constants are essentially determined by the inductive effect of the ring-substituent. The very similar slopes observed for the three plots (ρ comprised between 0.52 and 0.64) indicate that the substituents exert comparable effects on the ET reactions of the different ferrocene donors.

Calculations[30] using dispersion-correcting potentials[31] were performed to explore the π-stacked encounter complexes formed between the 4-X-CumO$^\bullet$ radicals and DcMFc. It is important to note that we did not search conformational space to find the

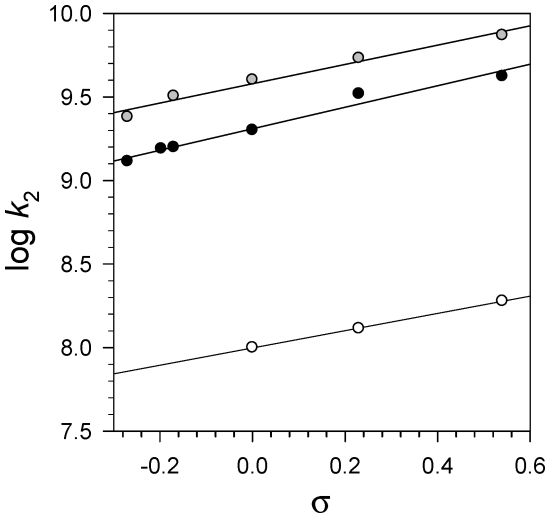

Figure 2. Dependence of the second-order rate constant (k_2) on the Hammett σ substituent constant for the reactions of 4-X-CumO$^\bullet$ with Me_nFc. From the linear regression analysis DMFc (open circles) ρ = 0.52, r^2 = 0.9996; OMFc (black circles) ρ = 0.64, r^2 = 0.9734; DcMFc (gray circles) ρ = 0.58, r^2 = 0.9736.

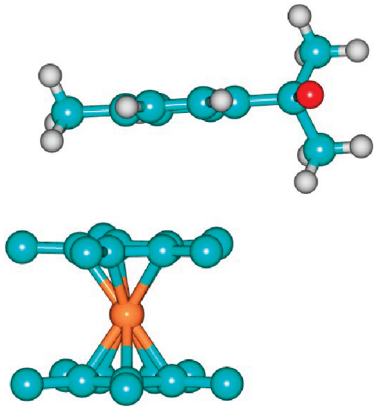

Figure 3. Optimized structure of the DcMFc/4-Me-CumO$^\bullet$ encounter complex. The intracomplex $\pi-\pi$ distance between the nearest aromatic rings of the two moieties is 4.1 Å. Key: blue = carbon, orange = iron, red = oxygen, white = hydrogen. The methyl hydrogens on DcMFc have been omitted for clarity.

global minimum encounter complex structure. However, our previous work showed that interactions between the aromatic ring of the arylcarbinyloxyl radical and the side of DcMFc is higher in energy than the π-stacked arrangement. Figure 3 shows the structure of the encounter complex between DcMFc and 4-Me-CumO$^\bullet$, which is characteristic of all the DcMFc/4-X-CumO$^\bullet$ complexes. As an additional example, the structure of the DcMFc/4-*t*-Bu-CumO$^\bullet$ encounter complex is shown in the Supporting Information (Figure S17).

Our calculations predict that the DcMFc/4-X-CumO$^\bullet$ encounter complexes are all strongly bound. Binding energies (BE) for X = CF_3, Cl, H, Me, *t*-Bu, and OMe are 7.5, 6.2, 5.4, 6.2, 6.5, and 6.8 kcal/mol, respectively. Note that all substituents, regardless of ED or EW character, increase the BE. A very similar trend in BEs was predicted for π-stacked C_6H_5X/C_6H_6 complexes using high-level wave function methods,[32] and was explained by an analysis of the balance between electrostatic and dispersion

dx.doi.org/10.1021/jo102420p |*J. Org. Chem.* 2011, 76, 1789–1794

forces. As was predicted for the ET reactions between alkylferrocenes and BnO$^{\bullet}$, the reactions involving substituted CumO$^{\bullet}$ are facilitated by the strong π-stacking: overlap of the aromatic rings provides a conduit for the electron being transferred between the Fe and the formal oxygen atom radical centers. However, despite the indication of very similar reduction potentials for BnO$^{\bullet}$ and 4-CF_3−CumO$^{\bullet}$ (see Table 1),[28] an up to 3-fold decrease in rate constant has been observed on going from the former radical to the latter one. In our previous modeling on the DcMFc/BnO$^{\bullet}$ π-stacked complex, the C−O bond was found to be oriented perpendicular to the plane of the aromatic ring.[17] This arrangement allows for optimal (but weak) conjugation of the formal, singly occupied O *p*-orbital with the BnO$^{\bullet}$ ring and ensures that the electron transferred from the DcMFc Fe center pairs up with the (formal) unpaired electron on the O atom. In the most stable conformation of the 4-X-CumO$^{\bullet}$/DcMFc encounter complexes, the C−O bond is essentially parallel to the plane of the aromatic ring. However, the facile rotation about the Ar−$C(CH_3)_2O^{\bullet}$ bond allows for optimal overlap to be achieved. This likely contributes, even though to a small degree, to the kinetic barrier of the ET reactions involving 4-X-CumO$^{\bullet}$/DcMFc systems.

The similar BEs and intracomplex $\pi-\pi$ distances obtained for the encounter complexes are in full agreement with the kinetic data displayed in Table 1, that show identical values of k_2 for the reactions of 4-Me-CumO$^{\bullet}$ and 4-*t*-Bu-CumO$^{\bullet}$ with OMFc. This indicates that the effect of the *t*-Bu substituent is essentially inductive in nature, as these two substituents are characterized by very close σ values (− 0.170 and −0.197, respectively)[29] and that steric effects due to the presence of the bulky *t*-Bu substituent do not play any significant role on the ET process.

The formation of strongly bound π-stacked encounter complexes has been previously observed by Kochi and co-workers for the ET reactions between alkylaromatic donors (ArH) and photoactivated quinone acceptors (Q*).[33,34] The authors observed that increases in the donor−acceptor distance caused by steric hindrance in the donor induce a changeover in the ET mechanism owing to the substantial decrease in the extent of donor/acceptor orbital overlap. Accordingly, with unhindered donors significant electronic coupling between donor and acceptor can be achieved, leading to tight complexes characterized by interaction energies significantly greater than 1 kcal/mol and donor/acceptor separations ≤4 Å. Under these conditions, deviations from the Marcus equation were observed and the reactions were described in terms of a (nonbonded) inner-sphere ET process characterized by the formation of a discrete encounter complex preceding the ET transition state (eq 3).

$$Q^* + ArH \overset{K_{EC}}{\rightleftarrows} [Q^*, ArH] \overset{k_{ET}}{\rightarrow} Q^{-\bullet} + ArH^{+\bullet} \qquad (3)$$

With hindered donors, weak coupling between donor and acceptor was observed leading to interaction energies ≤1 kcal/mol and donor/acceptor separations ≥4.5 Å. Under these conditions, the predicted Marcus outer-sphere ET behavior was observed.

Significantly higher ET rate constants were observed for the unhindered donor/acceptor couples as compared to the hindered ones, indicating that tight encounter complexes must experience a significant predisposition toward ET, which allows even endergonic ET reactions to occur at rate constants that approach the diffusion limit. The strong electronic coupling between the donor and the acceptor, as is indicated by the small separation, results in adiabatic ET with unit probability and therefore very high rate constants for (endergonic) inner-sphere ET.[33,35]

Along this line, the computed π-stacked encounter complexes between the 4-X-CumO$^{\bullet}$ radicals and DcMFc are characterized by separations around 4 Å and interaction energies on the order of 6 kcal/mol. Moreover, the measured second-order rate constants for the (endergonic) ET reactions of the 4-X-CumO$^{\bullet}$/Me_nFc couples approach in all cases the diffusion limit ($k_2 \geq 1.0 \times 10^9$ M^{-1} s^{-1}). These observations strongly support the hypothesis that the reactions between 4-X-CumO$^{\bullet}$ radicals and Me_nFc can also be described according to eq 3 in terms of a (nonbonded) inner-sphere ET mechanism that proceeds through the reversible formation of a complex followed by ET within the complex (eq 4).[36,37]

$$4\text{-X-CumO}^{\bullet} + Me_nFc \overset{K_{EC}}{\rightleftarrows} [4\text{-X-Cumo}^{\bullet}, Me_nFc] \overset{k_{ET}}{\rightarrow} 4\text{-X-Cumo}^{-} + Me_nFc^{+} \qquad (4)$$

This hypothesis is in line with our previous observation that the ET reactions of BnO$^{\bullet}$ and CumO$^{\bullet}$ with ferrocene donors do not follow a Marcus-type behavior.[17] Additional experimental and computational studies with highly hindered ferrocene donors may provide useful mechanistic information on the role of structural effects on these ET reactions.

EXPERIMENTAL SECTION

Materials. Spectroscopic-grade acetonitrile was used in the kinetic experiments. Commercial samples of 1,1′-dimethylferrocene (DMFc), 1,1′,2,2′,3,3′,4,4′-octamethylferrocene (OMFc), and decamethylferrocene (DcMFc) were of the highest commercial quality available (≥99%) and were further purified by sublimation prior to use. *tert*-Butyl 4-X-cumyl peroxides (X = Me, OMe, Cl, CF_3) were available from a previous work.[20] The synthesis of *tert*-butyl 4-*tert*-butylcumyl peroxide is described in the Supporting Information.

Laser Flash Photolysis Studies. LFP experiments were carried out with a laser kinetic spectrometer using the fourth harmonic (266 nm) of a Q-switched Nd:YAG laser, delivering 8 ns pulses. The laser energy was adjusted to ≤10 mJ/pulse by the use of the appropriate filter. A 3 mL Suprasil quartz cell (10 mm × 10 mm) was used in all experiments. Nitrogen-saturated acetonitrile solutions of *tert*-butyl 4-X-cumyl peroxides (between 2 and 10 mM) were employed. These peroxide concentrations were chosen in order to ensure prevalent absorption of the 266 nm laser light by the precursor peroxides in the presence of the ferrocene donors. All the experiments were carried out at $T = 25.0 \pm 0.5$ °C under magnetic stirring. First-order or pseudo-first-order rate constants were obtained by averaging four to eight individual values and were reproducible to within 5%.

The photochemical stability of the ferrocene donors at the laser excitation wavelength (266 nm) was checked by LFP of acetonitrile solutions containing donor concentrations comparable to the highest concentrations employed in the kinetic experiments. No evidence for the photolytic decomposition of the ferrocene donors or for the formation of the pertinent ferrocenium ions was obtained in these experiments.

Second-order rate constant for the reactions of the cumyloxyl radicals with the ferrocene donors (Me_nFc) were obtained from the slopes of the k_{obs} (measured following the buildup of the ferrocenium ion band between 300 and 330 nm, and with the 4-methoxycumyloxyl radical also

by following the decay of the visible absorption band at 580 nm) vs [Me$_n$Fc] plots.

Fresh solutions were used for every Me$_n$Fc concentration. Correlation coefficients were in all cases >0.992. The given rate constants are the average of at least two independent experiments, typical errors being <10%.

■ ASSOCIATED CONTENT

Supporting Information. Details of the synthesis of *tert*-butyl 4-*tert*-butylcumyl peroxide. NMR spectra. Time-resolved absorption spectra. Plots of k_{obs} vs [Me$_n$Fc] for the reactions of the 4-X-CumO$^•$ with the Me$_n$Fc. Plots of log k_2 vs EA (4-X-CumO$^•$). Computational details and data for the 4-X-CumO$^•$−DcMFc complexes and the electron affinities of 4-X-CumO$^•$. This material is available free of charge via the Internet at http://pubs.acs.org.

■ AUTHOR INFORMATION

Corresponding Author

*E-mail: bietti@uniroma2.it; gino.dilabio@nrc.ca; osvaldo.lanzalunga@uniroma1.it.

■ ACKNOWLEDGMENT

Financial support from the Ministero dell'Istruzione dell'Università e della Ricerca (MIUR) is gratefully acknowledged. We thank Lorenzo Stella for the use of LFP equipment and Alessandra Gentili for performing an Enhanced Resolution ESI(+) experiment.

■ REFERENCES

(1) Jomová, K.; Kysel, O.; Madden, J. C.; Morris, H.; Enoch, S. J.; Budzak, S.; Young, A. J.; Cronin, M. T. D.; Mazur, M.; Valko, M. *Chem. Phys. Lett.* **2009**, *478*, 266–270.

(2) Goldstein, S.; Samuni, A. *J. Phys. Chem. A* **2007**, *111*, 1066–1072.

(3) Fukuzumi, S.; Shimoosako, K.; Suenobu, T.; Watanabe, Y. *J. Am. Chem. Soc.* **2003**, *125*, 9074–9082.

(4) (a) Brinck, T.; Lee, H.-N.; Jonsson, M. *J. Phys. Chem. A* **1999**, *103*, 7094–7104. (b) Jonsson, M. *J. Phys. Chem.* **1996**, *100*, 6814–6818.

(5) (a) Das, T. N.; Dhanasekaran, T.; Alfassi, Z. B.; Neta, P. *J. Phys. Chem. A* **1998**, *102*, 280–284. (b) Alfassi, Z. B.; Khaikin, G. I.; Neta, P. *J. Phys. Chem.* **1995**, *99*, 265–268.

(6) Jovanovic, S. V.; Jankovic, I.; Josimovic, L. *J. Am. Chem. Soc.* **1992**, *114*, 9018–9021.

(7) Litwinienko, G.; Ingold, K. U. *Acc. Chem. Res.* **2007**, *40*, 222–230.

(8) Steenken, S.; Neta, P. In *The Chemistry of Phenols*; Rappoport, Z., Ed.; John Wiley & Sons: New York, 2003; Chapter 16, pp 1107−1152.

(9) Itoh, S.; Kumei, H.; Nagatomo, S.; Kitagawa, T.; Fukuzumi, S. *J. Am. Chem. Soc.* **2001**, *123*, 2165–2175.

(10) Armstrong, D. A.; Sun, Q.; Schuler, R. H. *J. Phys. Chem.* **1996**, *100*, 9892–9899.

(11) (a) Baciocchi, E.; Bietti, M.; Lanzalunga, O.; Lapi, A.; Raponi, D. *J. Org. Chem.* **2010**, *75*, 1378–1385. (b) Baciocchi, E.; Bietti, M.; Di Fusco, M.; Lanzalunga, O.; Raponi, D. *J. Org. Chem.* **2009**, *74*, 5576–5583. (c) Baciocchi, E.; Bietti, M.; Di Fusco, M.; Lanzalunga, O. *J. Org. Chem.* **2007**, *72*, 8748–8754.

(12) Galli, C.; Gentili, P.; Lanzalunga, O. *Angew. Chem., Int. Ed.* **2008**, *47*, 4790–4796.

(13) (a) Blinco, J. P.; Hodgson, J. L.; Morrow, B. J.; Walker, J. R.; Will, G. D.; Coote, M. L.; Bottle, S. E. *J. Org. Chem.* **2008**, *73*, 6763–6771. (b) Manda, S.; Nakanishi, I.; Ohkubo, K.; Yakumaru, H.; Matsumoto, K.; Ozawa, T.; Ikota, N.; Fukuzumi, S.; Anzai, K. *Org. Biomol. Chem.* **2007**, *5*, 3951–3955.

(14) Shao, J.; Geacintov, N. E.; Shafirovich, V. *J. Phys. Chem. B* **2010**, *114*, 6685–6692.

(15) (a) Magri, D. C.; Workentin, M. S. *Chem.—Eur. J.* **2008**, *14*, 1698–1709. (b) Donkers, R. L.; Workentin, M. S. *J. Am. Chem. Soc.* **2004**, *126*, 1688–1698. (c) Donkers, R. L.; Tse, J.; Workentin, M. S. *Chem. Commun.* **1999**, 135–136.

(16) (a) Donkers, R. L.; Maran, F.; Wayner, D. D. M.; Workentin, M. S. *J. Am. Chem. Soc.* **1999**, *121*, 7239–7248. (b) Antonello, S.; Musumeci, M.; Wayner, D. D. M.; Maran, F. *J. Am. Chem. Soc.* **1997**, *119*, 9541–9549. (c) Workentin, M. S.; Maran, F.; Wayner, D. D. M. *J. Am. Chem. Soc.* **1995**, *117*, 2120–2121.

(17) Bietti, M.; DiLabio, G. A.; Lanzalunga, O.; Salamone, M. *J. Org. Chem.* **2010**, *75*, 5875–5881.

(18) LFP of *tert*-butyl 4-X-cumyl peroxides also produces the *tert*-butoxyl radical (*t*-BuO$^•$). This radical, however, does not interfere with our measurements because, as mentioned above, the ET rate constants for its reaction with the ferrocene donors are at least 2 orders of magnitude lower than those measured for the corresponding reactions of CumO$^•$.[17]

(19) (a) Avila, D. V.; Ingold, K. U.; Di Nardo, A. A.; Zerbetto, F.; Zgierski, M. Z.; Lusztyk, J. *J. Am. Chem. Soc.* **1995**, *117*, 2711–2718. (b) Avila, D. V.; Lusztyk, J.; Ingold, K. U. *J. Am. Chem. Soc.* **1992**, *114*, 6576–6577.

(20) Baciocchi, E.; Bietti, M.; Salamone, M.; Steenken, S. *J. Org. Chem.* **2002**, *67*, 2266–2270.

(21) Baciocchi, E.; Bietti, M.; Lanzalunga, O.; Steenken, S. *J. Am. Chem. Soc.* **1998**, *120*, 11516–11517.

(22) Frey, J. E.; Du Pont, L. E.; Puckett, J. J. *J. Org. Chem.* **1994**, *59*, 5386–5392.

(23) Becke, A. D. *J. Chem. Phys.* **1993**, *98*, 5648–5652.

(24) Lee, C.; Yang, W.; Parr, R. G. *Phys. Rev. B* **1988**, *37*, 785–789.

(25) This model was described in: DiLabio, G. A.; Pratt, D. A.; LoFaro, A. D.; Wright, J. S. *J. Phys. Chem. A* **1999**, *103*, 1653–1661.

(26) Cossi, M.; Rega, N.; Scalmani, G.; Barone, V. *J. Comput. Chem.* **2003**, *24*, 669–681 and references cited therein.

(27) Gaussian 03, Revision D.01: Frisch, M. J.; Trucks, G. W.; Schlegel, H. B.; Scuseria, G. E.; Robb, M. A.; Cheeseman, J. R.; Montgomery, J. A., Jr.; Vreven, T.; Kudin, K. N.; Burant, J. C.; Millam, J. M.; Iyengar, S. S.; Tomasi, J.; Barone, V.; Mennucci, B.; Cossi, M.; Scalmani, G.; Rega, N.; Petersson, G. A.; Nakatsuji, H.; Hada, M.; Ehara, M.; Toyota, K.; Fukuda, R.; Hasegawa, J.; Ishida, M.; Nakajima, T.; Honda, Y.; Kitao, O.; Nakai, H.; Klene, M.; Li, X.; Knox, J. E.; Hratchian, H. P.; Cross, J. B.; Adamo, C.; Jaramillo, J.; Gomperts, R.; Stratmann, R. E.; Yazyev, O.; Austin, A. J.; Cammi, R.; Pomelli, C.; Ochterski, J. W.; Ayala, P. Y.; Morokuma, K.; Voth, G. A.; Salvador, P.; Dannenberg, J. J.; Zakrzewski, V. G.; Dapprich, S.; Daniels, A. D.; Strain, M. C.; Farkas, O.; Malick, D. K.; Rabuck, A. D.; Raghavachari, K.; Foresman, J. B.; Ortiz, J. V.; Cui, Q.; Baboul, A. G.; Clifford, S.; Cioslowski, J.; Stefanov, B. B.; Liu, G.; Liashenko, A.; Piskorz, P.; Komaromi, I.; Martin, R. L.; Fox, D. J.; Keith, T.; Al-Laham, M. A.; Peng, C. Y.; Nanayakkara, A.; Challacombe, M.; Gill, P. M. W.; Johnson, B.; Chen, W.; Wong, M. W.; Gonzalez, C.; Pople, J. A. Gaussian, Inc., Pittsburgh PA, 2004.

(28) We have recently shown that the difference in the calculated solvent-phase EAs between CumO$^•$ and *t*-BuO$^•$ (ΔEA(CumO$^•$ − *t*-BuO$^•$)) parallels the analogous $\Delta E°$ values.[17] Accordingly, by taking into account the reduction potential of CumO$^•$ ($E°_{CumO•/CumO-}$ = −0.19 V/SCE in MeCN),[16a] the ΔEA values obtained from Table 1 can provide reasonable estimates of the $E°$ values of the 4-X-CumO$^•$ radicals.

(29) Swain, C. J.; Lupton, E. C., Jr. *J. Am. Chem. Soc.* **1968**, *90*, 4328–4337.

(30) Using the B971 functional: Hamprecht, F. A.; Cohen, A. J.; Tozer, D. J.; Handy, N. C. *J. Chem. Phys.* **1998**, *109*, 6264–6271 as implemented in ref 27, along with 6-31+G(d,p) basis sets.

(31) (a) DiLabio, G. A. *Chem. Phys. Lett.* **2008**, *455*, 348–353. (b) Mackie, I. D.; DiLabio, G. A. *J. Phys. Chem. A* **2008**, *112*, 10968–10976.

(32) Sinnokrot, M. O.; Sherrill, C. D. *J. Am. Chem. Soc.* **2004**, *126*, 7690–7697.

(33) Hubig, S. M.; Rathore, R.; Kochi, J. K. *J. Am. Chem. Soc.* **1999**, *121*, 617–626.

(34) For a critical discussion of the role of structural effects on the ET reactions of π-stacked systems, see: Rosokha, S. V.; Kochi, J. K. *J. Am. Chem. Soc.* **2007**, *129*, 3683–3697.

(35) Marcus, R. A.; Sutin, N. *Biochim. Biophys. Acta* **1985**, *811*, 265–322.

(36) In ref 33, the kinetic plots of k_{obs} vs [ArH] for unhindered donors showed an asymptotic behavior diagnostic of a preequilibrium step that precedes ET. From these plots the preequilibrium constant (K_{EC}) and the intrinsic ET rate constant (k_{ET}) could be obtained. Linear plots of k_{obs} vs [Me_nFc] have been instead obtained for the reactions of the 4-X-CumO$^{\bullet}$ radicals, where the relatively strong absorption of the ferrocene donors at the laser excitation wavelength limited the study to [Me_nFc] $\leq$ 5 mM (see the Supporting Information). Accordingly, at these low concentrations the measured second order rate constant can be expressed as $k_2 = K_{EC}k_{ET}$. On the basis of this kinetic scheme, and on the data collected in Table 1, spectral evidence for the formation of an encounter complex would require significantly higher concentrations of the ferrocene donors. See, for example: Rathore, R.; Hubig, S. M.; Kochi, J. K. *J. Am. Chem. Soc.* **1997**, *119*, 11468–11480.

(37) A similar inner-sphere mechanism has been proposed for the ET reactions of the carbonate radical anion ($CO_3^{\bullet-}$) with oligonucleotides and of the nitrate radical ($NO_3^{\bullet}$) with alkylaromatic compounds. See: Lee, Y. A.; Yun, B. H.; Kim, S. K.; Mergolin, Y.; Dedon, P. C.; Geacintov, N. E.; Shafirovich, V. *Chem.—Eur. J.* **2007**, *13*, 4571–4581. Del Giacco, T.; Baciocchi, E.; Steenken, S. *J. Phys. Chem.* **1993**, *97*, 5451–5456.